

Numerical microcanonical ensemble method for calculation on statistical models with large lattice sizes

Jone-Zen Wang and Tzong-Jer Yang

Department of Electrophysics, National Chiao-Tung University, Hsinchu, Taiwan, Republic of China

(Received 22 January 1996; revised manuscript received 25 July 1996)

Based on the microcanonical ensemble theory in statistical mechanics, we devise a method that can be used to enhance the capability of numerical calculation on statistical models with large lattice sizes. In our method, we take the expectation value of the energy, as defined in quantum mechanics, instead of the eigenvalue as the energy of a physical system. We show mathematically that the relevant physical quantities obtained in this way are unchanged in the thermodynamical limit and we apply this method to numerical calculations. In this paper, we present our numerical results with the one-dimensional spinless fermionic model as a first test of our method. The numerical calculations are done to a 4096 lattice size using a computer with a speed of about 40 mflops. Our numerical data agree quite well with the exact values. Also, the fluctuation of data is small, in contrast to that obtained using the quantum Monte Carlo method. [S0163-1829(96)06143-7]

I. INTRODUCTION

In recent decades, physicists have been forced to face more and more complicated physical problems. The methods used to solve these problems also get more and more difficult. Several important theoretical models devised in recent years, such as the t - j model¹⁻³ and the Hubbard model^{4,5} in research on high- T_c superconductivity and the Anderson model^{6,7} in research on heavy fermions, invite many people to attempt a number of different methods to solve them. Among all the various approaches to these models, the analytical methods, such as exact solutions or perturbation theory, do give us some valuable insight into the physical meanings hidden in complicated systems with nonnegligible electron-electron interaction strength. But physicists still confront many unsolved problems in these models. Therefore, approximation methods play another important role in recent research into these models. But, as is well known, the results of approximation methods sometimes lead to doubtful conclusions. It is difficult to confirm which results obtained from approximation methods are reliable. To prevent these drawbacks inherent in analytical and approximation methods, numerical methods are frequently used. The most often used numerical skills at present are exact diagonalization methods; for example, the Lanczos algorithm⁸ and quantum Monte Carlo algorithms.^{3,9} But it is quite difficult to do calculations on large lattices. The largest lattice sizes ever reported in the literature on the calculation of the Hubbard model are, respectively, 10 and 256 (two-dimensional 16×16 lattice) for exact diagonalization methods and quantum Monte Carlo algorithms. Thus, in exact diagonalization methods, such a small lattice size cannot give satisfactory answers for most physicists. For Monte Carlo simulations, the lattice size used is larger, but still it does not seem large enough to ensure that the size effect can be safely neglected. Besides, the well known "sign" problem in fermionic models in quantum Monte Carlo simulations still cannot be treated satisfactorily, and this could affect the low-temperature results.

In order to overcome the handicaps encountered in numerical calculation, we propose a numerical microcanonical-ensemble method. In our method, expected values of the energy, instead of eigenvalues, are used in the calculation of microcanonical-ensemble theory. The related definition of entropy is also slightly modified. In a later section, we will prove that these definitions of energy and entropy are valid at the thermodynamical limit. With our method, we can do calculations on a large lattice, for example a 4096-site lattice. In this paper, our numerical calculations are done on a one-dimensional spinless fermionic model as a test of our method. The results that emerge seem quite reasonable. As to two-dimensional models, we are now modifying and testing the numerical program. Because the program is quite large, we need a lot of time to complete two-dimensional testing. We will present these results at a later time.

The primary requirements for our method to be usable on computers are large disk memory space and fast cpu speed. For one-dimensional models, the disk space needed is several hundred megabytes. For two-dimensional models, the disk space needed could be from several to 10 gigabytes. The computational time is acceptable for one-dimensional models. For the one-dimensional spinless fermionic model, it takes 2-3 cpu days to complete each calculation on a 40-mflops computer. For the two-dimensional spinless fermionic model, or bosonic model, the computational time may be 7-10 cpu days.

The remainder of this paper is organized as follows. In Sec. II, we prove our method mathematically. In Sec. III, we give a detailed description of how to apply our method to numerical calculation. In Sec. IV, we use exact results for the one-dimensional spinless fermionic model to check our numerical data. In Sec. V, we draw our conclusions.

II. THEORETICAL BACKGROUND

In statistical mechanics, when we use the microcanonical-ensemble method to evaluate physical quantities, we must first derive the relationship between entropy S and energy E . There are three equivalent ways¹⁰ to calculate S : (1) to

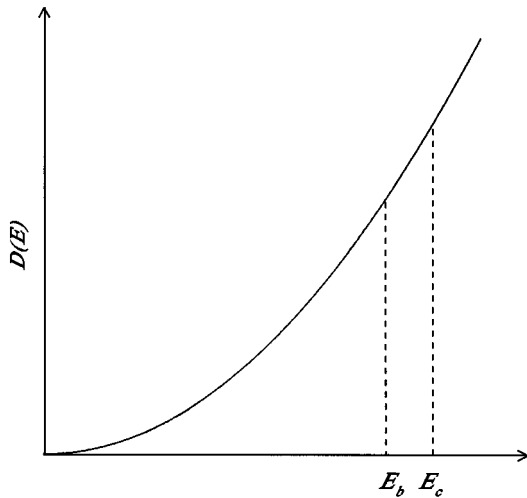


FIG. 1. Density of states as a function of energy.

evaluate the density of states $D(E)$; (2) to evaluate $P(E)$, which is defined as the total number of eigenstates whose energies are between E and $E + \delta$, δ being a small value; (3) to evaluate $\Sigma(E)$, which is defined as the total number of eigenstates whose energies are less than E . The definitions of entropy in these three cases are $S \equiv k \ln D(E)$, $S \equiv k \ln P(E)$ and $S \equiv k \ln \Sigma(E)$, respectively. At the thermodynamical limit, these three definitions are equivalent. Nevertheless, definition (3) is more often used because it is easier to evaluate $\Sigma(E)$ than either $P(E)$ or $D(E)$. But in practice $\Sigma(E)$ can be calculated only in very few statistical models, which means that the microcanonical-ensemble method is rarely used.

The difficulty encountered in evaluating $\Sigma(E)$ is that we must calculate all the eigenvalues of a complete many-particle system, but the number of eigenvalues is too large to be treated by any analytical or numerical methods. For example, there are about 10^{18} eigenstates in a 64-site lattice. So, our method is aimed at simplifying the way in which $\Sigma(E)$ is evaluated. Since the calculation of eigenvalues is always difficult, in our method we do not calculate eigenvalues directly. Rather, we hope that the expectation value of the energy $E = \langle \psi | H | \psi \rangle$ may be used to define $\Sigma(E)$. In the following paragraphs, we will show that it is valid to do this at the thermodynamical limit.

Now we give our proof. In Fig. 1 we define

$$\frac{\int_0^{E_c} E D(E) dE}{\int_0^{E_c} D(E) dE} \equiv E_b, \quad (1)$$

where $D(E)$ is the density of states. The scheme of our proof is first to show that the maximum number of states obeying the condition $\langle \varphi | H | \varphi \rangle = E_b$ is $\int_0^{E_c} D(E) dE$, and then to prove that $E_b \approx E_c$ and $\ln \int_0^{E_c} D(E) dE \approx \ln \int_0^{E_c} D(E) dE$.

In our proof, we will make use of the following lemma:

Lemma: If $\varphi_1, \varphi_2, \varphi_3, \dots, \varphi_n$, are orthonormal eigenstates of the Hamiltonian H , then we can combine these eigenstates linearly to construct new orthonormal states $\varphi'_1, \varphi'_2, \varphi'_3, \dots, \varphi'_n$ that obey the condition

$$\langle \varphi'_i | H | \varphi'_i \rangle = \bar{E}, \quad i = 1, 2, 3, \dots, n,$$

where

$$\bar{E} \equiv \frac{\sum_{i=1}^n \langle \varphi_i | H | \varphi_i \rangle}{n}.$$

The above lemma may be proved by the induction method. First, we consider that there are only two orthonormal states, say φ_a and φ_b with expected values of energy $E_a = \langle \varphi_a | H | \varphi_a \rangle$ and $E_b = \langle \varphi_b | H | \varphi_b \rangle$. Then it is simple to show algebraically that we can always combine φ_a and φ_b linearly to form new orthonormal states φ'_a and φ'_b , so that

$$\langle \varphi'_a | H | \varphi'_a \rangle + \langle \varphi'_b | H | \varphi'_b \rangle = E_a + E_b \quad (2)$$

and

$$E_{\min} \leq \langle \varphi'_a | H | \varphi'_a \rangle, \quad \langle \varphi'_b | H | \varphi'_b \rangle \leq E_{\max}, \quad (3)$$

where E_{\min} is the minimum of E_a and E_b and E_{\max} is the maximum of E_a and E_b . The above proof is valid whether or not φ_a and φ_b are eigenstates of the Hamiltonian H . So, when there are only two eigenstates, the lemma can be proved. Now we will prove that if the lemma is true for the number of eigenstates n , then it also holds for the $n + 1$ case. Consider that there are n orthonormal states $\varphi_1, \varphi_2, \varphi_3, \dots, \varphi_n$, whose expected energy values are all equivalent to \bar{E} . Then, when a new orthonormal state, say φ_{n+1} , with the expected energy value $E_{n+1} = \langle \varphi_{n+1} | H | \varphi_{n+1} \rangle$, is included in these n orthonormal states, the new average energy, defined as \bar{E}' , will be

$$\bar{E}' = \frac{n\bar{E} + E_{n+1}}{n+1}. \quad (4)$$

As shown in the proof for Eqs. (2) and (3), we can combine φ_1 and φ_{n+1} linearly to form new orthonormal states φ'_1 and $\varphi_{n+1}^{(1)}$ so that $\langle \varphi'_1 | H | \varphi'_1 \rangle = \bar{E}'$ and $\langle \varphi_{n+1}^{(1)} | H | \varphi_{n+1}^{(1)} \rangle = E_{n+1} + \bar{E} - \bar{E}'$. Then, we combine $\varphi_{n+1}^{(1)}$ and φ_2 linearly to form new orthonormal states $\varphi_{n+1}^{(2)}$ and φ'_2 so that $\langle \varphi'_2 | H | \varphi'_2 \rangle = \bar{E}'$ and $\langle \varphi_{n+1}^{(2)} | H | \varphi_{n+1}^{(2)} \rangle = E_{n+1} + 2(\bar{E} - \bar{E}')$. In the same way, we obtain final orthonormal states $\varphi'_1, \varphi'_2, \varphi'_3, \dots, \varphi'_n, \varphi_{n+1}^{(n)}$ such that

$$\langle \varphi'_i | H | \varphi'_i \rangle = \bar{E}', \quad i = 1, 2, 3, \dots, n \quad (5a)$$

and

$$\langle \varphi_{n+1}^{(n)} | H | \varphi_{n+1}^{(n)} \rangle = E_{n+1} + n(\bar{E} - \bar{E}'). \quad (5b)$$

Using Eq. (4), we can rewrite Eq. (5b) as

$$\langle \varphi_{n+1}^{(n)} | H | \varphi_{n+1}^{(n)} \rangle = \bar{E}'. \quad (5c)$$

So, the lemma is proven.

Besides the above lemma, we will also make use of the fact that the density of states $D(E)$ is an increasing function for almost all systems. The exceptional cases are finite-band systems whose $D(E)$ may possess a maximum point. But even in these cases, the behavior of $D(E)$ when $D(E)$ is a decreasing function of E is similar to (like a mirror image) that of $D(E)$ when it is an increasing function of E . So, we can simply consider $D(E)$ as an increasing function of E .

With this property and the above lemma, we can easily prove the following statement: The ‘‘maximum’’ number of states that obey the condition $\langle \varphi | H | \varphi \rangle = E_b$ is $\int_0^{E_c} D(E) dE$, where E_b and E_c are as defined in Eq. (1), because the definition of entropy is $S(E) \equiv k \ln \int_0^E D(E') dE'$. The key point to be stressed is that if E_c and E_b , as defined above, are close enough so that

$$\frac{|E_c - E_b|}{|E_c|} \ll 1 \quad (6a)$$

and

$$0 \ll \frac{\ln[(\int_0^{E_c} D(E) dE)/(\int_0^{E_b} D(E) dE)]}{\ln(\int_0^{E_c} D(E) dE)} \ll 1, \quad (6b)$$

then these two definitions of entropy, $S_c \equiv k \ln \int_0^{E_c} D(E) dE$ and $S_b \equiv k \ln \int_0^{E_b} D(E) dE$, are equivalent at the thermodynamical limit. That is, we can take E_b rather than E_c as the definition of energy and take the maximum number of states complying with the condition $\langle \varphi | H | \varphi \rangle = E_b$, denoted as $\Sigma'(E_b)$, to define the new entropy to be $S'_b \equiv k \ln \Sigma'(E_b)$. As shown in the above paragraphs, $S'_b = S_c$. Then, it is also reasonable to use the newly defined E_b and S'_b to evaluate any statistical quantities. Nevertheless, we must be aware that in most physical systems we are not able to evaluate the maximum value of the number of states obeying the condition $\langle \varphi | H | \varphi \rangle = E_b$. The value of the number of states we can actually calculate is always smaller than its maximum value $\Sigma'(E_b)$. But due to the logarithmic function in the definition of the entropy, we know that as long as the calculated value of the number of states is not much smaller than $\Sigma'(E_b)$, the calculated statistical properties should still be correct.

To give a clear illustration of the relationship between E_b , E_c , $\Sigma(E_c)$, and $\Sigma(E_b)$, we use the classical ideal gas¹⁰ as an example, because the closed form of $\Sigma(E)$ is known. It is

$$\Sigma(E) = C_{3N} [(V/h^3)(2mE)^{3/2}]^N, \quad (7)$$

where C_{3N} is a constant, m is the mass of one gas molecule, V is the volume, and N is the number of gas molecules. The density of states is

$$D(E) = \partial \Sigma(E) / \partial E = (3N/2E) \Sigma(E) \quad (8a)$$

and

$$\int_0^E \epsilon D(\epsilon) d\epsilon = \int_0^E \epsilon \frac{\partial \Sigma(\epsilon)}{\partial \epsilon} d\epsilon = \frac{(3/2)N}{(3/2)N+1} E \Sigma(E), \quad (8b)$$

$$\int_0^{E_b} (\epsilon - E_b) D(\epsilon) d\epsilon = \frac{-1}{(3/2)N+1} E_b \Sigma(E_b), \quad (8c)$$

$$\int_{E_b}^{E_c} (\epsilon - E_b) D(\epsilon) d\epsilon = \frac{1}{(3/2)N+1} E_b \Sigma(E_b) + \left(\frac{(3/2)N}{(3/2)N+1} E_c - E_b \right) \Sigma(E_c). \quad (8d)$$

If Eq. (8c) plus Eq. (8d) is equal to zero, then the following equation,

$$\frac{\int_0^{E_c} \epsilon D(\epsilon) d\epsilon}{\int_0^{E_c} D(\epsilon) d\epsilon} = E_b, \quad (9)$$

is correct, which means E_b is the average energy of all the eigenstates whose eigenvalues are less than E_c . Because Eq. (8c) plus Eq. (8d) equal zero, we get

$$E_c = E_b \left(\frac{(3/2)N+1}{(3/2)N} \right) = E_b + \frac{E_b}{(3/2)N}. \quad (10)$$

Then,

$$\Sigma(E_c) = C_{3N} [(V/h^3)(2m)^{3/2}]^N E_b^{(3/2)N} \left(1 + \frac{1}{(3/2)N} \right)^{(3/2)N} \xrightarrow{N \rightarrow \infty} e \Sigma(E_b). \quad (11)$$

That is, the maximum number of states complying with the condition $\langle \varphi | H | \varphi \rangle = E_b$ is $e \Sigma(E_b)$, so that the entropy

$$S_c \equiv k \ln \Sigma(E_c) = k \ln [e \Sigma(E_b)] = k + k \ln \Sigma(E_b) \approx k \ln \Sigma(E_b) \equiv S_b. \quad (12)$$

In the above example, the primary reason that our definition of energy and entropy is correct is that $\Sigma(E) \propto E^{\beta N}$; here, β may be a constant or a function of E , and N is the number of particles, which is always a very large number. Because entropy is an extensive thermodynamical quantity, β has a finite value and β/N must tend to zero when N is very large. So we can always find a macroscopically small but microscopically large value δ such that

$$\frac{|\delta|}{|E|} \ll 1, \quad (13a)$$

where the ground-state energy is set equal to zero and

$$(E + \delta)^{\beta N} \gg E^{\beta N}. \quad (13b)$$

So,

$$\Sigma(E + \delta) \gg \Sigma(E), \quad (14a)$$

$$D(E + \delta) \gg D(E). \quad (14b)$$

It is just this property that makes E_b and E_c , as defined in Eq. (9), very close, and makes $\Sigma(E_c)$ not much larger than $\Sigma(E_b)$. The reason is that we can approximate Eq. (9) as

$$\frac{E_c [\Sigma(E_c) - \Sigma(E_b)] + E_b \Sigma(E_b)}{\Sigma(E_c)} \approx E_b. \quad (15)$$

It can be seen that if $\Sigma(E_c) \gg \Sigma(E_b)$, the above equation cannot be satisfied. In quantum systems, the $\Sigma(E)$ may be of a more complicated form, such as $\Sigma(E) \propto [f(E)]^{\beta N}$, where $f(E)$ is a function of E , while the fact that $\Sigma(E)$ increases very fast with E is similar to that in the classical ideal gas. So, the proof in quantum systems follows straightforwardly.

III. ALGORITHM

In the numerical calculation, the primary scheme of our method is to calculate exact eigenvalues and eigenvectors when the lattice size is small, for example, a fermionic model with eight lattice sites. At this step, the periodic boundary condition is not suitable and the boundary condition we choose is that particles cannot hop outside the lattice. The number of particles in the lattice can be from 0 to 8. In each case, eigenstates and eigenvalues must all be calculated. Besides, the hopping and interacting, matrix elements must also be calculated in each case. These are, respectively, $\langle \varphi_{n+1,E'} | C_i^+ | \varphi_{n,E} \rangle$ and $\langle \varphi_{n,E'} | C_i^+ C_i | \varphi_{n,E} \rangle$, where C_i is an annihilation operator and C_i^+ is a creation operator, i denotes the lattice point near the boundary, and n is the number of particles. $|\varphi_{n,E}\rangle$ is the eigenstate whose energy is E and number of particles is n .

Then, the task is to merge two smaller lattices into a larger one, for example, merging two 8-site lattices into a 16-site lattice. In this step, the situation in which the final number of particles in a newly merged larger lattice is composed of different combinations of number of particles in the smaller lattices before merging must be taken into account. For example, if the number of particles in a 16-site lattice is 10, then the number of particles in those two 8-site lattices may be 2 and 8 or 3 and 7 or 4 and 6 or 5 and 5. Also, the interaction between these newly constructed states must be considered. For example, due to the hopping terms in the Hamiltonian, the states composed of 2 and 8 particles in the two smaller lattices before merging may interact with those states composed of 3 and 7 particles in the two smaller lattices. Similarly, through interacting terms in the Hamiltonian, the new states, whose numbers of particles in the two smaller lattices are 3 and 7, will interact with each other. So, at this step we also need to re-diagonalize the new Hamiltonian matrices that result from the merging of lattices.

The subsequent work in the numerical calculation is to use the hopping and interacting matrix elements to repeat the above procedures to merge lattices until the lattice is large enough. When merging proceeds, the total number of states increases very fast, far beyond that which can be treated by computer. Then we begin to collect those states with nearby energy as a bundle of states, and we use such bundles of states as quasistates to continue the process of merging lattices. So, at each step of our numerical calculation the norm of bundles of states, $\langle \varphi | \varphi \rangle$, and the expected energy values of bundles of states, $E = \langle \varphi | H | \varphi \rangle / \langle \varphi | \varphi \rangle$, must be evaluated. Certainly, $\Sigma(E)$ are also known.

Because of our use of bundles of states, people may wonder if our numerical algorithm is a mean-field method. We must stress that the use of bundles of states is due to the finite capability of computers. The situation is similar to that when we do numerical integration, where we can only divide the integration range into finite, but not infinite, small sec-

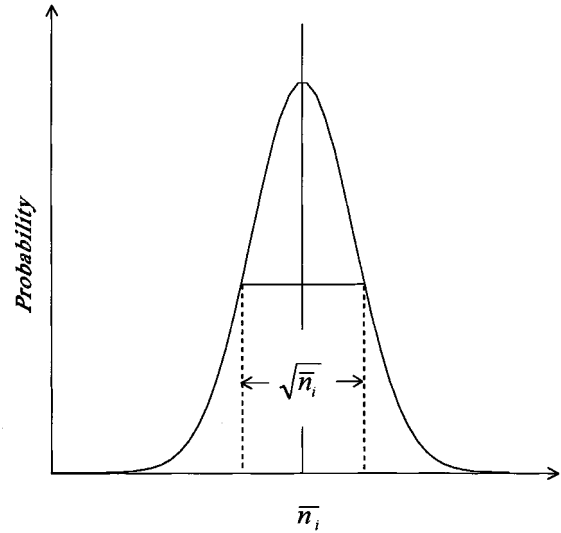


FIG. 2. Probability distribution function as a function of number of particles. \bar{n}_i is the most probable number of particles.

tions and sum the average function value in each small section to obtain the final integration value. Collecting states into bundles certainly introduces a mean-field effect, but such an effect is very much like that introduced in numerical integration. So the number of bundles of states used in our method controls the degree of accuracy that we can acquire. The numerical data shown in later sections are obtained with numbers of bundles of states at 65–80, and the energy deviation of our data from the exact value is about 2%, just as expected.

One point we want to stress is that, owing to the use of bundles of states, the number of states $\Sigma(E)$ evaluated in our numerical algorithm is not the same as the $\Sigma(E_c)$ in the proof of the preceding section. Nevertheless, the $\Sigma(E_c)$ is a limiting value. As long as the number of bundles of states used is increased, the $\Sigma(E)$, which is calculated in our numerical method, will get closer and closer to the limiting value $\Sigma(E_c)$.

In this algorithm, another problem that must be faced is that, in the process of merging two smaller lattices into a bigger one, we must know all the hopping and interacting matrix elements of those two smaller lattices, which are calculated for all cases of different numbers of particles in the lattices, before merging. For example, when we merge two 256-site lattices into a 512-site lattice, we must calculate all the hopping and interacting matrix elements of those two 256-site lattices within which the particle number ranges from 0 to 256. This is beyond the capability of the computer at the present time, so we use the root-mean-square deviation,¹¹ as defined in statistical mechanics, as a judgment of how to choose a cutoff value to reduce the range of particle numbers needed. See Fig. 2, in which

$$\langle n_i^2 \rangle - \langle n_i \rangle^2 \approx \bar{n}_i, \quad (16)$$

where \bar{n}_i is the mean particle number. So, in the numerical algorithm, we calculate the matrix elements with a particle number of $\bar{n}_i \pm \sqrt{\bar{n}_i}/2$. In our calculation, \bar{n}_i is set to the value which is decided in the final step of the merging.

Now we give a more detailed discussion of how to calculate the energy of each bundle of states and the maximum value of $\Sigma(E)$ as demanded in the proof in the preceding section. The procedure is simply to make the variation

$$\delta \left(\frac{\langle \varphi | H | \varphi \rangle}{\langle \varphi | \varphi \rangle} \right) = 0, \quad (17)$$

where $\langle \varphi | \varphi \rangle$ need not be 1. So, the mathematical manipulation is identical to that of eigenvalue problems. The eigenvalue problem directly implies that the evaluated $\Sigma(E)$ is a maximum value in our numerical scheme. The reason is that if we sum the lowest n eigenvalues to evaluate their average energy as \bar{E}_n , then the maximum number of randomly chosen eigenstates with their average energy equivalent to \bar{E}_n must be n .

As we have mentioned above in the second paragraph of this section, at each step of the merging lattice, we must also re-diagonalize the new Hamiltonian matrix. But, at later steps of the process of merging lattices, the norm $\langle \varphi | \varphi \rangle$ of bundles of states increases very fast with increasing energy of the bundles of states. So, in order to evaluate the energies of bundles of states as accurately as possible, we must construct the new Hamiltonian suitably and evaluate the energies of bundles of states. For example, consider the merging of two 32-site lattices to a 64-site lattice. We assume that the number of bundles of states to be used is 100; then there will be 10 000 new states formed each time two smaller 32-site lattices, which each have 100 bundles of states, are connected to a 64-site lattice. Different combinations of numbers of particles in the two smaller 32-site lattices may correspond to the same final number of particles in the 64-site lattice. So, for a given final number of particles, say 28, in the 64-site lattice, there may be as many as 10^5 new states formed in total. The Hamiltonian of these new states needs to be diagonalized to evaluate new eigenstates. But it takes a lot of computer time to diagonalize a matrix with dimensions as large as 10^5 . Furthermore, the subsequent work in evaluating the new hopping and interaction matrix elements consumes even more cpu time. So, we need to make some approximations. We rearrange and collect these newly constructed 10^5 states to about 100^2 states. In these 100^2 states, we arrange the states with nearby energies, which are meant to be the diagonal terms of the Hamiltonian matrix, so that they have the same norms. The number of these states, which have the same norms, is chosen to be about 100. We only diagonalize the Hamiltonian matrix of these 100 states at each stage. That is, we neglect the effect of the interaction of these 100 states with other states whose energies are beyond some cut-off value. After each stage of diagonalization calculation, we collect those states with eigenvalues near the lowest eigenvalue in that stage as the output to form the final bundles of states. Those states that are not chosen as the output of each diagonalization stage will be put into the next stage of calculation with other states whose energies are higher. Therefore, our numerical procedures for evaluating energies and norms of bundles of states are separated into many stages, and these stages are followed one by one over the whole energy range. So, besides the final number of bundles of states that we use, the dimension of the matrix used in each stage of the numerical diagonalization constrains the accu-

racy. The computational time grows as the fourth power of the dimension of the matrix. The dimension of the matrix that we use in the present work is about 100. If, in the future, the dimension of the matrix can be extended to several hundreds, the accuracy will be much better.

In our method, because the number of bundles of states and the dimension of the matrix used in evaluating the energy must be finite, some truncation effect exists. So, the two-particle correlation function cannot be calculated at too long a distance. In the future, when the speed of computers increases, the two-particle correlation function can be calculated at a longer distance also. In the one-dimensional spinless fermionic model, we find that the two-particle correlation function can be calculated up to about 20 lattice points apart.

IV. COMPARISON WITH EXACT RESULTS

To check the reliability of our numerical method, we calculate the statistical properties of the exactly solvable, one-dimensional, spinless fermionic model whose Hamiltonian is

$$H = \sum_{|i-j|=1} t C_i^+ C_j, \quad (18)$$

where the hopping parameter t is set to be 1 eV. C_i^+ and C_j are fermionic operators. The exact values of the specific heat and the density correlation functions $\langle n_0 n_r \rangle$, which are used as a check of our numerical results, are obtained from the canonical-ensemble calculations with lattice size equivalent to 10^5 .

Our numerical data are described below. In these data the lattice size is 4096.

(1) In Figs. 3 and 4, the low-temperature data of our numerical calculation are shown and compared with exact values. The procedure that we use to get the low-temperature properties of this model is to gradually discard the higher energy states as the merging of lattices proceeds. In Figs. 3(a) and 3(b), the data are obtained with a number of particles equivalent to 1024. Figure 3(a) shows the specific heat versus temperature behavior. The numerical scheme, which we use to evaluate the specific heat and temperature, is that first we use polynomials to fit the energy and entropy data and then take first and second derivatives of these polynomials to evaluate the temperature and specific heat. Figure 3(b) shows the behavior of the ground-state density correlation $\langle n_0 n_r \rangle$. Because the density correlation does not show apparent change at low temperatures, we only show the ground-state density correlation data. In Fig. 3(a), the ground-state energy we get is -1.77053 eV per particle and the exact value is -1.80044 eV per particle.

In Figs. 4(a) and 4(b), the number of particles is 2048. The ground-state energy we get is $-1.25 291$ eV per particle and the exact value is $-1.27 306$ eV per particle.

From these results we know that the energy deviation of our numerical data from exact values is 1.5–2 %; that is just as expected, because the number of bundles of states used in the calculation is about 85. In Fig. 4(a), the deviation of data is larger than that in Fig. 3(a) because the slope of the line in Fig. 4(a) is only one-third that in Fig. 3(a). Such a small slope means that the numerical calculation is about at the boundary of reasonable accuracy that we can acquire because

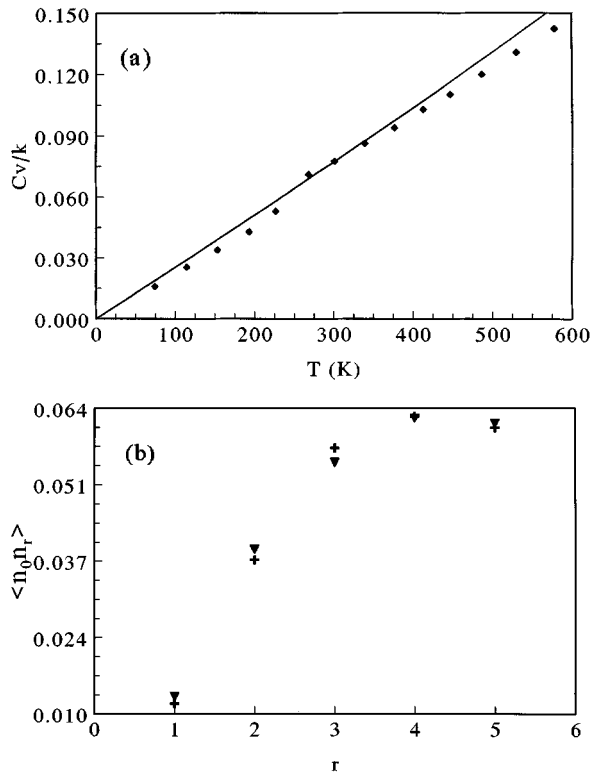


FIG. 3. (a) Specific heat over k as a function of temperature; the line shows the exact value and the squares show our data. (b) Ground-state density correlation $\langle n_0 n_r \rangle$ as a function of r ; the crosses show exact values and the triangles show our data. The particle density $\langle n \rangle$ is $\frac{1}{4}$ in (a) and (b).

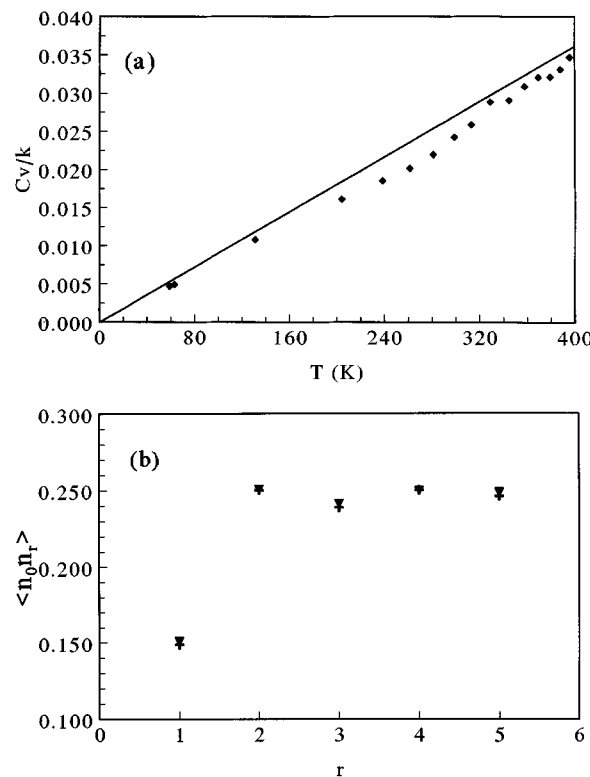


FIG. 4. Same as Fig. 3 except that particle density $\langle n \rangle = \frac{1}{2}$.

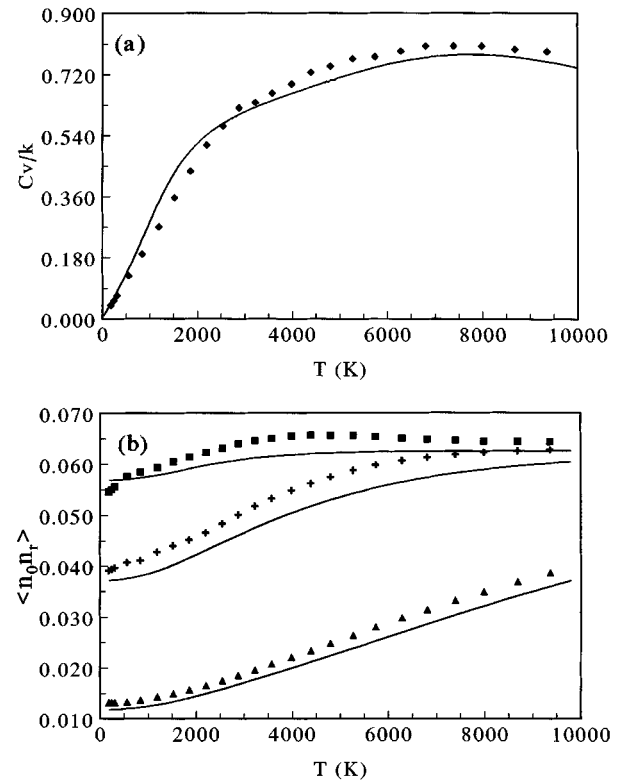


FIG. 5. (a) Specific heat over k as a function of temperature, the line shows the exact value and the squares show our data. (b) Density correlation $\langle n_0 n_r \rangle$ for $r=1, 2, 3$ as a function of temperature; the lines show exact values and our data are marked by triangles ($r=1$), crosses ($r=2$), and squares ($r=3$). The particle density $\langle n \rangle$ is $\frac{1}{4}$ in (a) and (b).

the hopping parameter is 1 eV and the particle number is 2048 and the number of bundles of states is about 85, which all constrain the accuracy in Fig. 4(a). Actually, when we calculate the data of Fig. 4(a) we focus on lower-energy states than when we calculate the data of Fig. 3(a). Furthermore, owing to the use of bundles of states, the norms of higher-energy states are larger than those of lower-energy states. The mean-field effect introduced is also larger in higher-energy states. Therefore, the lower-energy states can be evaluated more accurately. But the uncertainty principle tells us that the acceptable energy uncertainty is larger in higher-energy states, which means that the calculated high-temperature statistical properties may be more stable. So, it is reasonable to expect the larger data deviation to appear at the intermediate temperature range between about 200 and 300 K. The low-temperature data are nevertheless more stable. The first five data points in Fig. 4(a) change slightly, whether we use second-order or third-order polynomials to fit the corresponding energy and entropy data.

(2) Figures 5 and 6 show the high-temperature behaviors. The C_v/k -versus- T figures show that larger deviations from exact values should result from the numerical differentiation scheme because, as we have mentioned above, when we evaluate C_v data we must take second derivatives of the polynomials that are used to fit the energy and entropy data. The second derivatives are sensitive and prone to introducing larger deviations. Besides, the use of polynomials does not seem the best choice because some part of the data may be

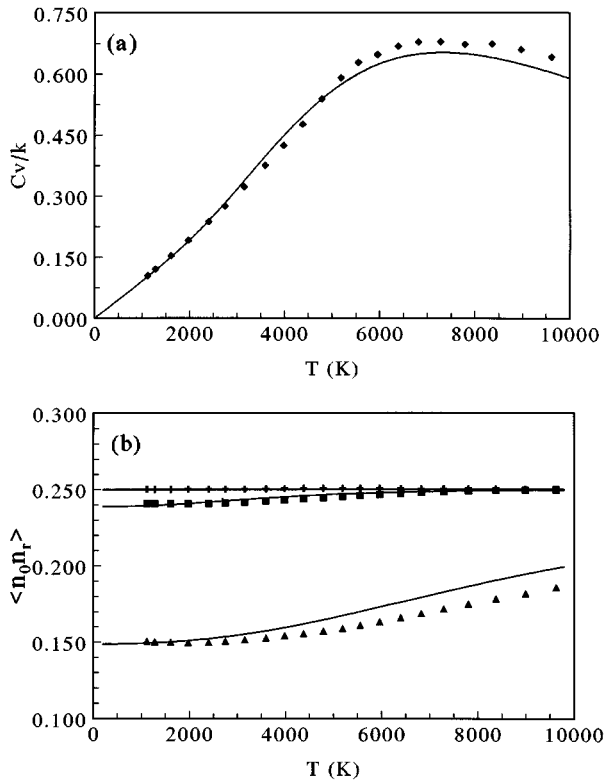


FIG. 6. Same as Fig. 5 except that particle density $\langle n \rangle = \frac{1}{2}$.

fitted well by lower-order polynomials but another part of the data may need higher-order polynomials to obtain a good fit. The reason we still use polynomials is that polynomials are sensitive enough for our data.

In Fig. 5(a), the deviation of data is larger than that in Fig. 6(a). The reason is that the slope of the curve in Fig. 5(a) changes quickly at about 2000 K, which tends to cause the wavy behavior of fitted polynomials.

(3) In Figs. 7(a) and 7(b), the data show the changes of ground-state density correlation functions as a function of lattice size L , which increases when the numerical steps of merging lattices proceed. These two figures are used to illustrate that our method really can reflect the effect of lattice size when the lattice gets larger and larger.

V. CONCLUSIONS AND REMARKS

Through the comparisons in one-dimensional data given in the preceding section, it seems that the outcomes of our numerical method agree well with exact values. This is powerful evidence that our numerical algorithm is trustworthy. Also, the lattice size that we use in the calculations is large enough to suggest that the size effect is not of practical importance. Besides, in all our numerical calculations, we find that the results obtained from our method are stable. For example, when evaluating the data of Fig. 4(a), if we make a cruder calculation, that is, if we use the same number of bundles of states to calculate the thermal properties at a wider range of temperatures, we still get the linear behavior

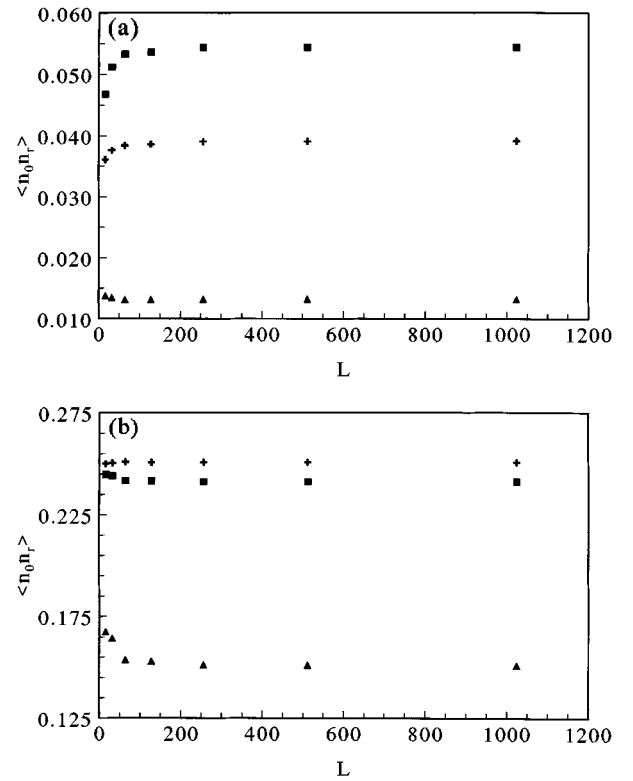


FIG. 7. (a) Ground-state density correlation $\langle n_0 n_r \rangle$ as a function of lattice size L when our numerical steps of the merging lattice proceed. The particle density $\langle n \rangle$ is $\frac{1}{4}$. The triangles are for $r=1$, the crosses are for $r=2$, and the squares are for $r=3$. (b) The same as (a) except that $\langle n \rangle = \frac{1}{2}$.

of C_v -versus- T data with the slope at about 80% that of the exact values. So, it seems that our method at least qualitatively shows the correct physical properties even when numerical results obtained from our method are quantitatively not so satisfactory.

Because the proof given in Sec. II is correct for any dimension, our method can also be applied to two- and three-dimensional models. Our plan for future work is to use this numerical method on two-dimensional models. But, in order to attain the same level of accuracy as in the one-dimensional results, the number of bundles of states used in the calculation on two-dimensional models must be larger. This means that the computational time needed is also much longer. So, for two-dimensional models, the numerical calculation is not easy. Anyway, to our approximation, once the speed of the computer is 10–20 times faster, the accuracy of our numerical calculation for two-dimensional models should be satisfactory. So, we think that in the future our method should be a trustworthy and not too difficult method for tackling one- and two-dimensional models.

ACKNOWLEDGMENTS

We would like to thank the National Science Council of R.O.C. for financial support through Grants Nos. NSC 84-2112-M-009-902-PH and NSC 85-2112-M-009-029-PH.

- ¹M. Ogata, M. Luchini, S. Sorella, and F. F. Assaad, *Phys. Rev. Lett.* **66**, 2388 (1991).
- ²Y. C. Chen, A. Moreo, F. Ortolani, E. Dagotto, and T. K. Lee, *Phys. Rev. B* **50**, 655 (1994).
- ³E. Dagotto, *Rev. Mod. Phys.* **66**, 763 (1994).
- ⁴E. Dagotto, F. Ortolani, and D. Scalapino, *Phys. Rev. B* **46**, 3183 (1992).
- ⁵J. A. Riera and E. Dagotto, *Phys. Rev. B* **50**, 452 (1994).
- ⁶R. M. Fye, *Phys. Rev. B* **41**, 2490 (1990).
- ⁷Zs. Gulacsi, R. Strack, and D. Vollhardt, *Phys. Rev. B* **47**, 8594 (1993).
- ⁸J. K. Cullum and R. A. Willoughby, *Lanczos Algorithms for Large Symmetric Eigenvalue Computations* (Birkhauser, Boston, 1985).
- ⁹E. Manousakis, *Rev. Mod. Phys.* **63**, 1 (1991).
- ¹⁰K. Huang, *Statistical Mechanics*, 1st ed. (Wiley, New York, 1963); 2nd ed. (Wiley, New York, 1987). The notations that we use are slightly different, with $\Gamma \rightarrow P$ and $\omega \rightarrow D$.
- ¹¹K. Huang, *Statistical Mechanics* (Ref. 10, 1st ed.), Eqs. (4.54) and (7.9).